Precision Determination of Photoneutron Thresholds*

MILTON BIRNBAUM†
Nucleonics Division, U. S. Naval Research Laboratory, Washington, D. C.
(Received August 6, 1953)

The photoneutron thresholds for C^{12}, N^{14}, O^{16}, Cu^{63}, and Ag^{109} were determined by measurement of the yield of activity as a function of the peak bremsstrahlung energy. Measurements of the photoneutron thresholds of C^{12}, N^{14}, and O^{16}, which could be calculated accurately from the mass data, served to determine the energy scale. The photoneutron thresholds for Cu^{63} and Ag^{109} were found to be 10.61 ± 0.05 Mev and 9.07 ± 0.07 Mev, respectively.

The shape of the activation curves for C^{12}, N^{14}, and O^{16} appeared to be a straight line for about 350 kev near threshold. The activation curves for Cu^{63} and Ag^{109} could be fitted accurately by functions of the form $Y=k(E-E_t)^{2.23}$ and $Y=k(E-E_t)^{1.90}$, respectively, over a 3-Mev interval. E refers to the peak x-ray energy and E_t to the threshold energy.

I. INTRODUCTION

THE measurement of the photoneutron reaction threshold provides a method for determining the neutron binding energy. For those reactions where the binding energy can be accurately calculated from a knowledge of the masses, the threshold for the reaction serves to determine the x-ray energy. In this way, an x-ray energy scale can be calibrated.

More detailed information about the activation curves in the neighborhood of threshold should indicate a method for unique extrapolation of the yield curve to zero yield. In addition, the shape of the activation curve in the neighborhood of threshold should provide information, in conjunction with other data, on the dependence of the cross section for the reaction on the x-ray energy. About 38 photoneutron thresholds had been determined relative to an energy scale based upon the Cu^{63} threshold of 10.9 ± 0.2 Mev.[1–8] In view of the widespread use of this value for the Cu^{63} threshold, it appeared desirable to obtain a more reliable value.

Thresholds may be determined by observing the yield of activity or neutrons[9] as a function of the peak x-ray energy. In the present work, thresholds were determined by the yield of activity. The thresholds of C^{12}, N^{14}, and O^{16}, which could be calculated from the mass data, were used to determine the energy scale of the betatron.

II. DESCRIPTION OF APPARATUS

The source of x-rays for these experiments was the U. S. Naval Research Laboratory 22-Mev betatron. The method used for control of the peak x-ray energy was similar to that described by Katz *et al.*[10] A diagram of the experimental arrangement is shown in Fig. 1.

The induced sample activity was counted by means of a Geiger tube (Amperex Beta Counter, No. 120C) and a scaling circuit. The output of the scaler was fed into a Streeter-Amet Company "Ametron" Counter. At preset time intervals ranging from 30 seconds to 12 hours, the number on its register, together with the date and time, could be printed on a paper tape. During the threshold determinations, the number of counts was recorded by the printing mechanism at one-minute intervals, synchronized with the electric clock used to time the irradiation of the sample.

All of the samples irradiated were in the form of disks of 1.750-in. diameter. The copper and silver disks were 0.040 in. thick, and the disks of polyethylene (C), boric acid (O), and melamine (N) were 0.125 in. thick. These thicknesses are of the order of the absorption length of the most energetic betas emitted on irradiation of the respective samples.[11] The disks were all machined to a 0.001 in. tolerance in all dimensions to render them as nearly identical (and therefore interchangeable) as possible.

As indicated in the diagram of Fig. 1, the disk was supported approximately tangent to the doughnut at the exit point of the x-ray beam. This geometry was advantageous in two ways. When the sample is placed as close as possible to the source of the x-rays, the irradiation is obtained at the highest available flux density. The activity counted originated mainly from the surface layer of the sample, and, in this geometry, the beam intercepted more of the surface layer.

The x-ray beam intensity and x-ray dosage were monitored by identical air ionization chambers posi-

* Abstracted from a thesis submitted to the University of Maryland in partial fulfillment of the requirements for the Ph. D. degree. Phys. Rev. **91**, 474A (1953).
† Now at Bulova Research and Development Laboratories, Bulova Park, Flushing 70, New York.
[1] G. C. Baldwin and H. W. Koch, Phys. Rev. **67**, 1 (1945).
[2] McElhinney, Hanson, Becker, Duffield, and Diven, Phys. Rev. **75**, 542 (1949).
[3] Hanson, Duffield, Knight, Diven, and Palevsky, Phys. Rev. **76**, 578 (1949).
[4] H. Palevsky and A. O. Hanson, Phys. Rev. **79**, 242 (1950).
[5] W. E. Ogle and R. E. England, Phys. Rev. **78**, 63 (1950).
[6] Ogle, Brown, and Carson, Phys. Rev. **78**, 63 (1950).
[7] R. W. Parsons and C. H. Collie, Proc. Phys. Soc. (London) **A63**, 839 (1950).
[8] Parsons, Lees, and Collie, Proc. Phys. Soc. (London) **A63**, 915 (1950).
[9] Sher, Halpern, and Mann, Phys. Rev. **84**, 387 (1951).
[10] Katz, McNamara, Forsyth, Haslam, and Johns, Can. J. Research **A28**, 113 (1950).
[11] E. Pollard and W. L. Davidson, Jr., *Applied Nuclear Physics* (John Wiley and Sons, Inc., New York, 1942), p. 228.

tioned as shown in Fig. 1. The ionization chambers were of conventional design, not hermetically sealed, and consisted of 3 parallel plates, of which the center plate was maintained at ground potential and the outside plates at about 320 volts above ground. The design incorporated a guard ring in order to reduce the effects of leakage current. The current produced by the x-ray beam in the ionization chamber most distant from the betatron (Fig. 1) was fed into a current integrator and indicator circuit. The basic circuit was that of a very stable direct-current amplifier.[12] The calibration was accomplished by comparison with the reading of a Victoreen Roentgen Meter at a peak x-ray energy of 20 Mev. The reading was obtained by means of a standard Victoreen thimble imbedded in the center of a 4-in. cubical block of Lucite. The absolute measurement of the number of roentgens was not required for these experiments.

Several improvements were incorporated in the electronic circuits for accurate control of the peak x-ray energy. The ac line voltage to the integrator amplifier was regulated with a Sorenson line voltage regulator which maintained the root-mean-square line voltage constant to within ± 0.1 percent. The reference voltage power supply was checked against a standard cell before and during an irradiation and maintained constant to within ± 0.01 percent. To achieve more stable triggering of the 5C22 injector and expander thyratrons, a trigger circuit consisting of a 2050 thyratron was employed. This circuit produced a pulse of over 200 volts across a 100-ohm load with a rise time of less than 0.01 microsecond and was used to trigger the 5C22 thyratrons.

About 60 watts were dissipated in the 1-megohm resistor of the integrator stack at a magnet amplitude corresponding to an energy of 21 Mev. Bench tests indicated a change in resistance of several tenths of a percent until thermal equilibrium was reached. In order to reduce variations in the peak x-ray energy caused by this effect, a circuit was designed and installed which put a 60-cycle voltage across the stack, equal to the 180-cycle voltage across the stack when the magnet amplitude was set for a peak x-ray energy of 21 Mev. By this means, the integrator stack was always maintained at an equilibrium condition for a 21-Mev magnet amplitude.

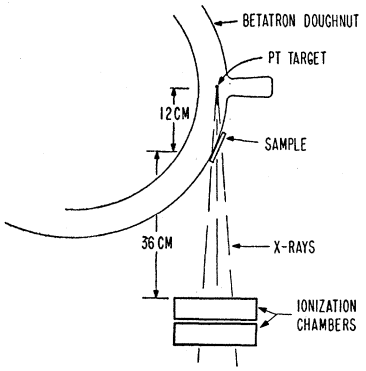

FIG. 1. Experimental arrangement.

[12] W. A. Higinbotham and S. Rankowitz, Rev. Sci. Instr. 22, 688 (1951).

III. EXPERIMENTAL TEST OF THE APPARATUS

In order to test the alignment of the sample with respect to the x-ray beam, the method of autoradiography was employed. Autoradiographs of the irradiated Cu disk showed blackening which indicated the position of the maximum intensity of the x-ray beam. The sample was then positioned so that the x-ray beam center coincided with the disk center.

The background counting rate was determined each day by the counts accumulated during the preceding 8 to 24 hours. A counting rate of about 21 counts per minute was usually obtained. The total variation in the background counting rate was less than ± 1 count per min over a 9-month interval. The entire apparatus for counting sample activity was tested daily by means of a standard beta-ray source. Over the 57 days during which most of the data presented in this paper were obtained, the total spread in the measurements was about ± 1.3 percent. However, all but six of the measurements fell within the limits of ± 0.7 percent. Thus, the long period reliability and reproducibility of the counting apparatus was ± 0.7 percent.

The factors which might produce errors in the measurement of the x-ray dosage were departure from linearity of the current integrator, drift of the amplifier of the current integrator, and the effect of variations in temperature and barometric pressure on the efficiency of the ionization chamber. It was concluded, after numerous tests, that the over-all long-time reliability of the instruments for measuring the x-ray dosage should be of the order of ± 1.8 percent. However, on any given day the fluctuations resulting from the aforementioned effects should be less than ± 1 percent.

The method of determination of an activation curve consists of a sequence of exposures of the samples at different peak x-ray energies. A procedure was adopted which would insure good reproducibility of the irradiation and counting schedules. In fact, the irradiation and counting schedules could be reproduced with an uncertainty of less than one second, which would produce a negligible effect on the induced radioactivity.

In order that the activities of the irradiated disks be directly comparable in terms of the number of roentgens received by the disk, it was necessary to insure that the intensity wave form of the irradiation be the same for all exposures. The simplest wave form to use was a square wave; that is, the flux of x-rays was maintained at a constant value during the irradiation. Ordinarily, it was found possible to keep the flux of x-rays constant to about ± 2 percent. Calculation of the uncertainty in the activations (expressed in counts per roentgen)

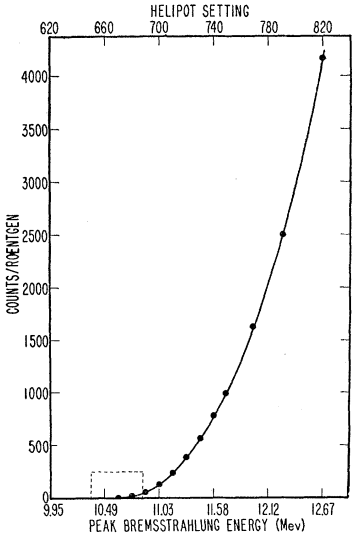

FIG. 2. Cu^{62} activation curve.

which resulted from variations in the wave form indicated that it was practically negligible.

Reproducibility of Activations

It had been realized throughout the course of this work that the peak x-ray energy of the betatron would be one of the most difficult factors to control with a high degree of stability over a long time interval. It was for this reason that several improvements, described above, were incorporated into the peak x-ray energy control circuits. In fact, the instability of the peak x-ray energy was one of the major factors which limited the precision of the threshold determinations in previous work.[1,2,9]

A test of the stability of the peak x-ray energy was obtained by the reproducibility of Cu activations at helipot 730, approximately 800 kev above the Cu^{63} gamma-neutron threshold. Reference to the activation curve of Fig. 2 indicated a slope of about 20 counts per roentgen per helipot unit.[13] Thus, at helipot 730 a change in the peak x-ray energy of 0.1 percent produced a 3.6 percent change in the Cu activity. A sequence of Cu disks was irradiated at a peak x-ray energy corresponding to helipot 730. The dispersion in the activations was a measure of the peak x-ray stability. For 11 irradiations of Cu at helipot 730, a spread in activity of 1.3 percent was recorded. The uncertainties due to statistics and other effects described above contributed 0.7 percent to the observed spread of activities. Thus, the spread in activity due to fluctuations of the peak x-ray energy was about 1.1 percent or 10 kev (0.8 h.u.) at a peak energy of 11.4 Mev. In most cases, the fluctuations of the peak x-ray energy during a day were somewhat greater, usually about ± 20 kev.

[13] The abbreviations c/r and h.u. will stand, respectively, for counts per roentgen and helipot unit.

Monitoring the Peak X-Ray Energy

Since at helipot 730 the largest uncertainty by far in the reproducibility of Cu activations was due to the peak x-ray energy fluctuation, for simplicity, from now on, all the observed changes in activity of Cu at helipot 730 will be ascribed to this cause. It is now evident that the activation of Cu at helipot 730 can be used to monitor the peak x-ray energy. Suppose, for example, that on one day the Cu control activity[14] was 600 c/r and on another 500 c/r. Reference to Fig. 2 shows that the peak x-ray energy has shifted by 5 h.u. To normalize the latter to the former, it would be necessary to subtract 5 h.u. It will be shown later that this method can be rigorously justified.

The Cu^{62} activation curve approximately 800 kev above threshold was determined when the control runs indicated a peak x-ray stability of 10 kev. This activation curve, free from distortions caused by fluctuations in the peak x-ray energy, was used throughout the threshold determinations to correct for fluctuations and shifts in the peak x-ray energy as indicated by the Cu control activity.

Experimental Procedure

A very sensitive test of sample purity from the point of view of a threshold determination could be obtained by plotting a decay curve of the induced activity. If the curve of log (counting rate) *versus* the time is accurately represented by a straight line, then it may be concluded that there is no, or very little, activity of other half-lives present. Furthermore, the agreement of the measured half-life with that given by other observers identified positively the nucleus under investigation. In all cases, the half-life measurements identified the reactions studied.

In each case, a standard irradiation and counting schedule was adopted. A series of runs at different peak x-ray energies was obtained; this constituted the data for the activation curve. Usually about three Cu control activations were obtained at the beginning of each day. If these showed good agreement, the threshold determination was started. A control run was taken for every one, two, or three data runs. The decision regarding the distribution of the control runs with respect to the data runs depended upon the agreement of the control runs.

IV. PHOTONEUTRON THRESHOLD DETERMINATIONS

Photoneutron Threshold of Cu^{63}

The standard exposure and counting schedule consisted of a 4-min irradiation and a 20-min counting interval, beginning 1.5 min after the x-ray bombardment. The Cu disks were supported during exposure by a holder which completely surrounded them with a

[14] Activity of Cu at helipot 730 for the purpose of monitoring the peak x-ray energy will be referred to as Cu control activity.

$\frac{1}{32}$-in. thickness of Cd. The x-ray dosage was about 100 r at one meter or about 5700 r at the sample position. For Cu irradiations at helipot settings above 730, both time of exposure to the x-ray beam and beam intensity were reduced to obtain initial counting rates less than 10 000 counts per minute. These runs were normalized to those obtained with the standard procedure.

The activation curve for the reaction $Cu^{63}(\gamma,n)Cu^{62}$ is shown in Fig. 2. The ordinates represent the observed activity in c/r corrected for cosmic-ray background and for the different exposure times. The dotted-line portion of Fig. 2 is shown on an expanded scale in Fig. 3. Inspection of the curve of Fig. 3 indicated threshold at 670±1 h.u. In Figs. 2 and 3 there is shown an upper abscissa scale in helipot units and a lower one in peak bremsstrahlung energy. The method of conversion of the arbitrary helipot unit scale to the peak x-ray energy scale will be described later.

Some of the points on the curve of Fig. 3 are represented by the intersection of a vertical and horizontal bar. The vertical bar represents the standard error in the c/r caused by counting statistics only. The horizontal bar represents the precision to which the helipot setting was known, as obtained from the Cu control runs. About 22 Cu control runs were obtained for the data shown in Figs. 2 and 3. Since most of the data near threshold were obtained with a Cu control of 565 c/r, all the data were referred to this value. The spread in the control activations was from 585 to 536 c/r or ±1.25 h.u.[15]

The presence of an appreciable activity below threshold is due to the reactions $Cu^{65}(\gamma,n)Cu^{64}$, $Cu^{65}(n,\gamma)Cu^{66}$, and $Cu^{63}(n,\gamma)Cu^{64}$. The Cu^{64} and Cu^{66} activities have 13-hour and 5-min half-lives, respectively. The contribution of the former was determined by counting the disks after the 10-min activity had practically disappeared. The Cu^{64} activity amounted to 0.15 c/r at helipot 670 and so contributed only a very small fraction of the observed activity. Analysis of the data taken at helipot settings below 670 (Fig. 3) indicated a 5-min half-life. The activity was therefore attributed to Cu^{66} through neutron capture in Cu^{65}.

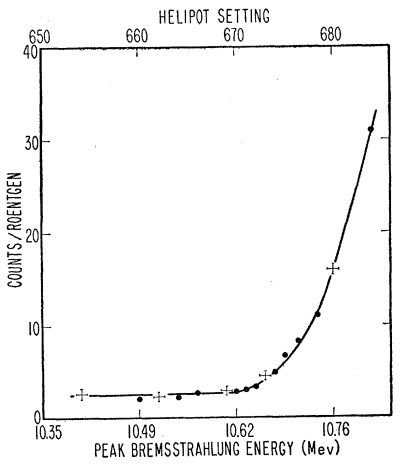

FIG. 3. Detail of Cu^{62} activation curve near threshold. The vertical bars represent the standard error caused by counting statistics only; the horizontal bars, the uncertainty in the helipot setting.

[15] One h.u. is equal to approximately 14 kev.

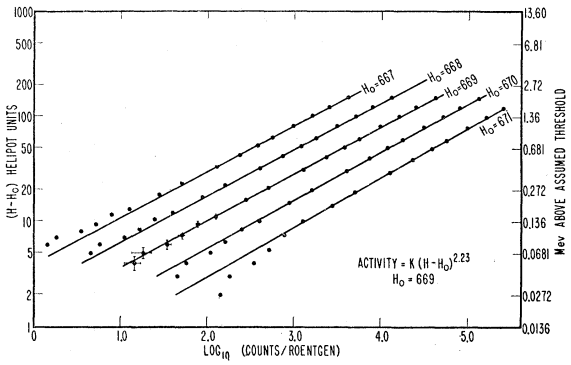

FIG. 4. Log-log graph of Cu^{62} activation curve of Figs. 2 and 3. The points for the line $H_0=667$ represent the $\log_{10}$ of the corrected activities. To the abscissas of the points for $H_0=668$ have been added 0.5; to those of $H_0=669$, 1.0; and so on. The horizontal bars represent the standard errors caused by counting statistics only; the vertical bars, the uncertainty in the helipot setting.

In Fig. 4 is shown the log-log analysis of the Cu^{62} activation curve shown in Figs. 2 and 3. The activities have been corrected by subtraction of the 13-hour and 5-min components. The points for the line $H_0=667$ represent the $\log_{10}$ of the corrected activities. However, to the abscissas of the points for $H_0=668$ have been added 0.5; to those of $H_0=669$, 1.0; and so on. This has been done in order to display on a single sheet the behavior of the log-log analysis as a function of the threshold parameter H_0. The log-log analysis is an attempt to fit the activation curve with a function of the form $Y=k(H-H_0)^x$. H_0 is said to be the threshold because the yield is zero when $H=H_0$. One of the main advantages of this type of analysis is the fact that the yield data are uniquely extrapolated to zero yield.

It is evident from Fig. 4 that the best fit to a straight line is obtained with $H_0=669$ and $x=2.23$. A choice of H_0 different by 1 h.u. from 669 results in a poorer fit to the data. The threshold was therefore taken to be 669±1 h.u., in agreement with that obtained by inspection of Fig. 3, 670±1 h.u. The agreement obtained with these two methods showed that practically no part of the activation curve near threshold was obscured by the residual activity. Similar results were obtained in two other determinations of the Cu^{63} threshold.

Photoneutron Threshold of Ag^{109}

A similar procedure was used in the threshold determination for Ag^{109}. Near threshold, each Ag disk was irradiated for 5 min, receiving about 4500 r. Counting was started 1 min after the exposure and terminated on the tenth minute.

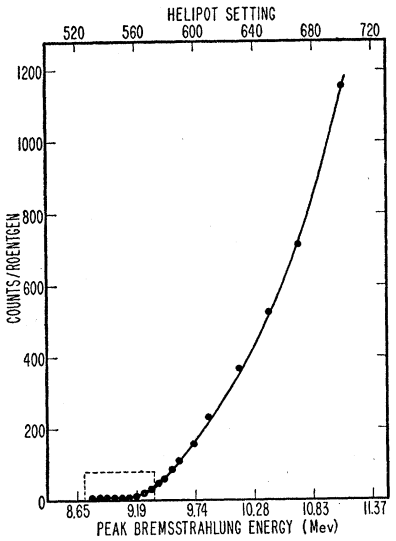

FIG. 5. Ag^{108} activation curve.

The data shown in the activation curve of Fig. 5 have been corrected for cosmic-ray background, the 24-min Ag^{106} activity, and the different irradiation times employed. The Ag^{106} activity was first observed about 330 kev above the Ag^{109} threshold. The portion of the activation curve enclosed in the dashed lines of Fig. 5 is shown enlarged in Fig. 6. Inspection of Fig. 6 indicated a threshold of 551 ± 1 h.u. It is apparent from Fig. 6 that there is a residual activity below threshold. This residual activity showed a half-life of about 2 min. The activity was assigned to Ag^{108} with a half-life of 2.4 min produced through neutron capture in Ag^{107}.

Most of the data near threshold were obtained with a Cu control of 680 c/r, and the threshold determination was referred to this Cu control activity. About 43 control runs were obtained during the 5-day interval occupied by the threshold determination. These showed a spread in activity of from 709 to 648 c/r or ±1.5 h.u.

The log-log analysis of the Ag^{108} activation data is shown in Fig. 7. The activities have been corrected by subtraction of the residual activity below threshold as

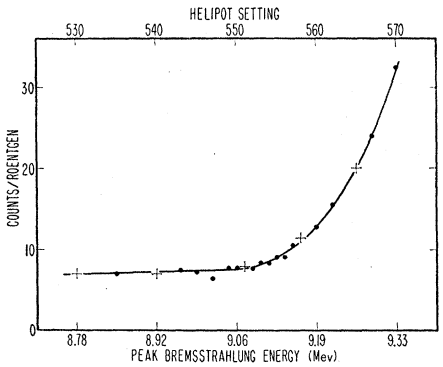

FIG. 6. Detail of Ag^{108} activation curve near threshold.

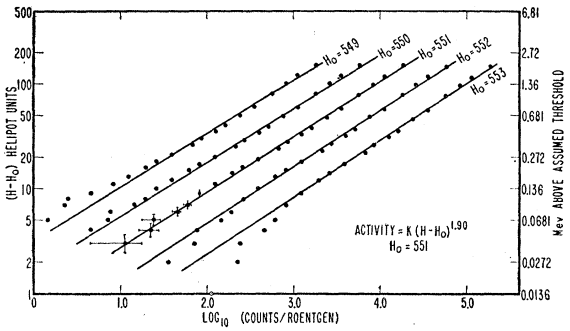

FIG. 7. Log-log graph of Ag^{108} activation curve of Figs. 5 and 6. The points for the line denoted by $H_0=549$ represent the $\log_{10}$ of the corrected activities $+0.2$; $H_0=550$, $+0.7$; $H_0=551$, $+1.2$; and so on.

discussed above. The line denoted by $H_0=549$ in Fig. 7 has abscissas which are $\log(c/r)+0.2$; $H_0=550$, $\log(c/r)+0.7$; $H_0=551$, $\log(c/r)+1.2$; and so on. As in the previous case, this is done in order to display the entire analysis on a single sheet. The threshold obtained by this method was 551 ± 1 h.u. in exact agreement with that obtained by inspection of the activation curve of Fig. 6.

Photoneutron Threshold of O^{16}

The procedure used was similar to that already described, except that the disks were not surrounded by cadmium during exposure. The exposure time was 4 min, during which the sample received about 13 000 r. It was counted for 10 min, starting 1 min after exposure. The activation curve is shown in Fig. 8. The portion enclosed by the dashed line is shown on an expanded scale in Fig. 9. It is seen on inspection of Fig. 9 that the threshold was at 1034 ± 1 h.u. The activation curve of

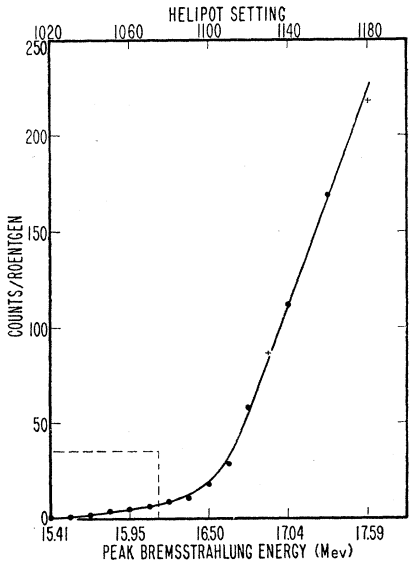

FIG. 8. O^{15} activation curve.

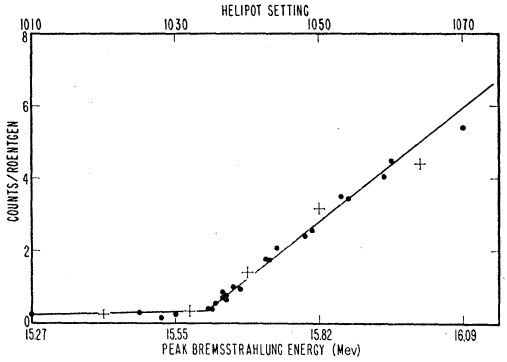

FIG. 9. Detail of O^{15} activation curve near threshold.

Fig. 9 showed that from helipot 1070 down to threshold (about 480 kev) the activation curve was linear. The intersection of this line with that determined by the points below helipot 1033 is used as the experimental definition of threshold for the reaction $O^{16}(\gamma,n)O^{15}$.

Analysis of the decay curves below threshold indicated that the residual activity had a 5–10-min half-life. Only about 50 counts were obtained, and the poor statistics prevented a more reliable determination. An analysis of the decay curves for a series of oxygen runs ranging from helipot 1040–1180 showed the 2-min O^{15} half-life.

Photoneutron Threshold of N^{14}

Among the various solid compounds containing a high percentage of N by weight, melamine, $C_3N_6H_6$, was chosen.[16] The procedure was similar to that employed in the O^{16} determination. The irradiation time was 15 min, during which time the disk received about

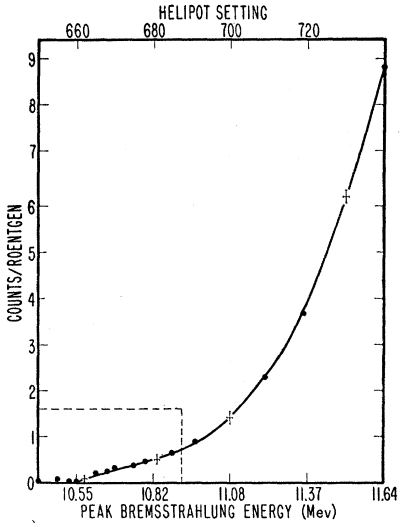

FIG. 10. N^{13} activation curve.

[16] The author wishes to thank the American Cyanamid Company for their cooperation in providing the pure malamine resin.

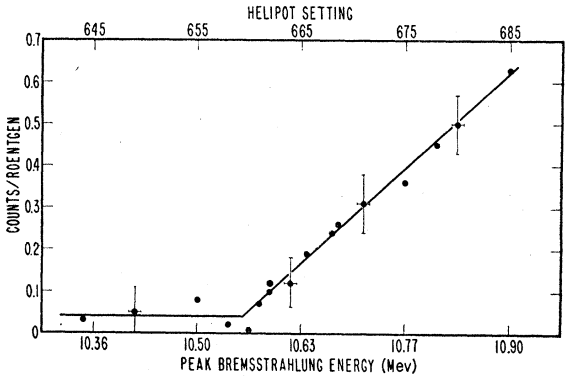

FIG. 11. Detail of N^{13} activation curve near threshold.

20 000 r. The "hot" melamine disk was counted for 30 min, starting 1.5 min after the exposure.

The activation curve for the reaction $N^{14}(\gamma,n)N^{13}$ is shown in Figs. 10 and 11. Inspection of Fig. 11 showed that from helipot 684 down to threshold (about 340 kev) the activation curve appeared linear. The threshold was determined by the intersection of this line with the line determined by the residual activity below threshold and was found to be 659±2 h.u. The activity of the runs below threshold was so weak that it was not possible to attempt a half-life analysis. On the average, 9 counts were recorded in the 30-min counting interval for the points below threshold. The data shown in Figs. 10 and 11 were referred to a Cu control of 710 c/r. About 25 Cu control runs were obtained, and these showed a spread in activities of 743 to 657 c/r or ±2.1 h.u.

Photoneutron Threshold of C^{12}

The procedure employed was similar to that described in connection with the O^{16} and N^{14} thresholds. Polyethylene disks were irradiated for 10 min, receiving about 35 000 r. The exposed disks were counted for 30 min, starting 1.5 min after irradiation.

The activation curve for the reaction $C^{12}(\gamma,n)C^{11}$ is

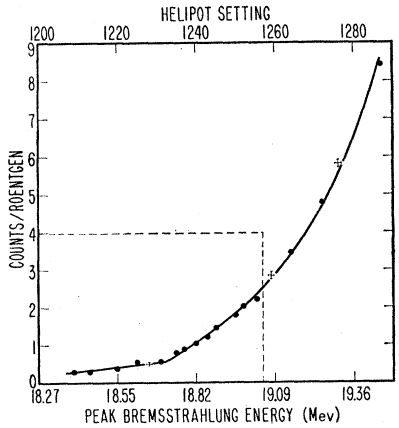

FIG. 12. C^{11} activation curve.

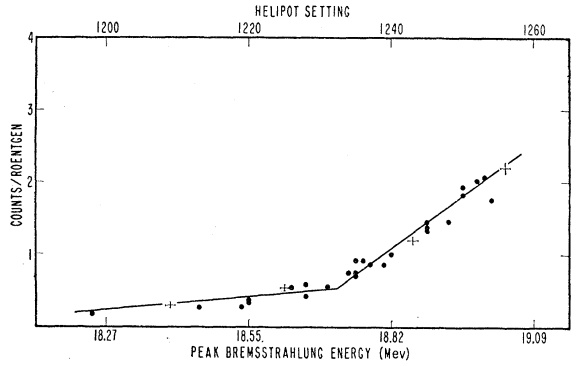

FIG. 13. Detail of C^{11} activation curve near threshold.

shown in Figs. 12 and 13. However, the activities plotted were for a 20-min counting interval beginning 11.5 min after irradiation and corrected for an equivalent 6-min exposure. The activation curve appeared linear (Fig. 13) from helipot 1255 down to threshold (about 310 kev). The threshold was determined by the intersection of this line with that determined by the points below threshold and was found to be 1232±2 h.u.

The activity represented by the points below helipot 1232, the C^{12} threshold, was the strongest encountered in any of the determinations. This was not too surprising, since the threshold of C^{12} occurs at about 18.7 Mev, which is well above the photoneutron threshold for practically all other nuclei. Furthermore, the slope of the background line indicated an activity which was strongly energy-dependent. In order to establish with greater certainty that helipot 1232 corresponded to the C^{12} threshold, a careful analysis of the half-lives of the activities, shown in Fig. 13, was performed. The activities below helipot 1232 had an average half-life of about 11 min and showed a sharp increase for higher helipot settings. The half-lives increased rapidly from 14 min at 1234 to 20 min at 1250. Thus, it appeared very likely that the sharp increase in activity at helipot 1232 was due to the onset of the 20-min C^{11} activity.

The residual activity below helipot 1232 was attributed to a very small nitrogen impurity producing the 10-min N^{13} activity. The cross section for the photoneutron reaction in N^{14} increases steeply in the region between 18 and 20 Mev,[17] and this could account for the energy dependence. It is now evident that a counting interval of from 11.5 to 31.5 min after irradiation is preferred to the 1.5- to 31.5-min interval, because the former interval discriminates more strongly against the 10-min activity as compared to the 20-min C^{11} activity.

V. SHAPE OF ACTIVATION CURVES NEAR THRESHOLD

It has been found that the photoneutron activation curves for Cu^{63} and Ag^{109} can be represented by a function of the form $Y=k(H-H_0)^x$ over a 3-Mev interval. These results agree qualitatively with those of other investigators. A comparison of the experimental results is shown in Table I.

The activation curves for C^{11}, N^{13}, and O^{15} over the measured intervals (0.8, 1.4, and 2 Mev, respectively) could not be represented by an expression of the form, $Y=k(H-H_0)^x$. In these cases, however, the activation curves near threshold appeared to be linear functions of the peak x-ray energy. For C^{11} and N^{13}, this region extended from threshold to about 340 kev above, and for oxygen to about 480 kev above threshold.[18] Thus, the shapes of the activation curves of the light nuclei were different from those of the medium-weight nuclei of Cu^{63} and Ag^{109}.

The above results for the light nuclei differ from those of other investigators. McElhinney *et al.*[2] found that the activation curves over a 3-Mev interval for all photoneutron reactions studied (including C^{12}, N^{14}, Cu^{63}) could be represented by a function, $Y=k(H-H_0)^2$. Sher *et al.*[9] found that, over a 3-Mev interval, the activation curves could be represented by a function, $Y=k(H-H_0)^x$, for all the photoneutron reactions (over 70) investigated. The exponent, x, varied from 0.7 to 3.1. In these experiments only a small number of data were obtained in the neighborhood of threshold.

TABLE I. Comparison of values of exponent.

Target nucleus	Exponent Birnbaum	McElhinney *et al.*[a]	Sher *et al.*[b]
Cu^{63}	2.23	2	1.5
Ag^{109}	1.90	2	2.5

[a] See reference 2.
[b] See reference 9.

Over a small energy interval, the response of the ion chamber x-ray monitors will be almost independent of the peak x-ray energy. Thus, for the light nuclei, where the shape of the activation curves over a 350-kev interval is considered, the variation of the monitor response should be negligible. However, over a 3-Mev interval, the shape of the activation curves may be somewhat dependent on the monitor response. No attempt was made to correct the results for the energy dependence of the x-ray monitor.

[17] Johns, Horsley, Haslam, and Quinton, Phys. Rev. **84**, 856 (1951).

[18] In several recent investigations, it has been found that the activation curves for the photoneutron reactions in O^{16}, C^{12}, Li^7, and F^{19} consisted of straight-line regions with sharp breaks. The sharp breaks were taken to represent energy levels in the target nucleus. It is possible that the activation curves for C^{11}, N^{13}, and O^{15} reported in this paper consist of straight-line regions with sharp breaks. However, the investigation has not been carried far enough in this direction to reach any conclusions. Haslam, Katz, Horsley, Cameron, and Montalbetti, Phys. Rev. **87**, 196 (1952). J. Goldemberg and L. Katz, Bull. Am. Phys. Soc. **28**, No. 4, 16 (1953). L. Katz and J. Goldemberg, Bull. Am. Phys. Soc. **28**, No. 4, 16 (1953).

VI. PHOTONEUTRON THRESHOLD VALUES FOR Cu^{63} AND Ag^{109}

From the mass data[19] (energy conservation calculation), the threshold energies for C^{12}, N^{14}, O^{16} were found to be 18.712±0.027, 10.545±0.017, and 15.597±0.012 Mev, respectively. To these energies must be added a small additional energy, required by momentum conservation considerations, which for C^{12}, N^{14}, O^{16} amounted to 0.016, 0.004, and 0.008 Mev. Thus, the calculated threshold energies were: C^{12}, 18.728±0.027 Mev; N^{14}, 10.549±0.017 Mev; O^{16}, 15.605±0.012 Mev.

The results of threshold determinations No. 1 (shown in Figs. 2–13) for C^{12}, N^{14}, O^{16}, Cu^{63}, and Ag^{109} were, respectively, 1232±2, 659±2, 1034±1, 662±1.5, and 550±1.5 h.u. referred to a Cu control of 710 c/r. A linear energy scale can be determined using any pair of threshold values for the light nuclei. Here, N^{14} is always used as one of the pair, since the thresholds to be determined were close to that of N^{14}. The results are summarized in Table II.

The results of threshold determinations No. 2 for C^{12}, N^{14}, O^{16}, Ag^{109} and Cu^{63}, referred to a Cu control of 480 c/r, were, respectively, 1243±2, 669±2, 1040±1, 562±1, and 674±1 h.u. These results are summarized in Table III. The corrections to the threshold values resulting from momentum conservation amounted to 0.001 and 0.0004 Mev for Cu^{63} and Ag^{109}, respectively, and were therefore neglected.

TABLE II. Thresholds based on N^{14}, O^{16}, C^{12} determinations No. 1.

Energy scale determination	Slope (kev/h. u.)	Threshold (Mev) Cu^{63}	Threshold (Mev) Ag^{109}
N^{14}, O^{16}	13.5	10.59±0.05	9.08±0.07
N^{14}, C^{12}	14.3	10.59±0.05	8.99±0.07

Although the respective threshold values quoted in Tables II and III have the same precision estimates, the results in Table III are considered to be somewhat more reliable than those of Table II, for the following reason. The total spread in the values of the Cu control activity was 516 to 466 c/r or ±0.017 Mev for the determinations of C^{12}, N^{14}, O^{16}, and Cu^{63}, so that corrections for shift of the peak x-ray energy were not required. The Ag^{109} threshold was referred to a Cu control of 520 c/r and was normalized to a Cu control of 480 c/r, the correction amounting to 0.027 Mev.

The fact that the slopes were different (Tables II and III) (N^{14} and O^{16} were used as scale-calibration points) from the slope determined by N^{14} and C^{12} was an indication of a nonlinearity in the relationship between helipot setting and peak x-ray energy. The nonlinearity, defined as the difference in slopes divided by the average slope, amounted to approximately 4 percent. This nonlinearity did not affect the threshold determination for Cu^{63} because its threshold is so close to that of N^{14}. However, in the case of Ag^{109}, the nonlinearity results in a greater uncertainty in the threshold determination. The value for the threshold of Ag^{109} was taken to be 9.07±0.07. This figure reflects the fact that more weight was given to the determinations using N^{14} and O^{16} than to those of N^{14} and C^{12}. This was reasonable, since the N^{14} and O^{16} calibration points are closest to the threshold of Ag^{109}. The average value for the threshold of Cu^{63} was found to be 10.61±0.05 Mev. A comparison of the threshold values obtained in this work as compared with those of other investigators[1,2,20,21] is shown in Table IV.

TABLE III. Thresholds based on N^{14}, O^{16}, C^{12} determinations No. 2.

Energy scale determination	Slope (kev/h.u.)	Threshold (Mev) Cu^{63}	Threshold (Mev) Ag^{109}
N^{14}, O^{16}	13.6	10.62±0.05	9.09±0.07
N^{14}, C^{12}	14.2	10.62±0.05	9.03±0.07

VII. PROOF OF METHOD OF Cu CONTROL ACTIVITY

A method of testing the absolute validity of the helipot correction method based upon the Cu control activity was afforded by the existence of two groups of threshold determinations, one obtained with a Cu control in the neighborhood of 710 c/r and the other with a control of 480 c/r. The method consists in comparing the change in threshold predicted by the Cu control data with the measured threshold changes. The comparison is tabulated in Table V below.

The first three sets of data offer the most significant proof of the method, since the nonlinearity of the scale will be insignificant over so small a range. It is evident that the numbers in column 4 and column 5 of Table V are in excellent agreement and thus establish the method on an absolute basis to a precision of about 0.9 h.u. This error was due mainly to uncertainties in the threshold measurements, most of which were determined to within 1 to 2 h.u. On a relative basis

TABLE IV. Cu^{63} and Ag^{109} threshold values.

Observer	Notes	Threshold values (Mev) Cu^{63}	Threshold values (Mev) Ag^{109}
Baldwin & Koch[a]		10.9 ±0.3	9.3 ±0.5
McElhinney *et al.*[b]	Compared to N^{14}	10.8 ±0.2[d]	
McElhinney *et al.*[b]	Av. of 3 diff. methods	10.9 ±0.2[e]	
Sher *et al.*[c]		10.85±0.2	9.05±0.2
Birnbaum		10.61±0.05	9.07±0.07

[a] See reference 1.
[b] See reference 2.
[c] See reference 9.
[d] See reference 20.
[e] See reference 21.

[19] Li, Whaling, Fowler, and Lauritsen, Phys. Rev. **83**, 512 (1951).

[20] The Cu^{63} threshold was referred to the N^{14} threshold of 10.55±0.02 Mev.

[21] The results of the three methods were: energy scale defined by thresholds of Be^{9} and C^{12}, 10.9±0.2 Mev; direct comparison with N^{14} threshold; measurement of magnetic field, 11.0±0.2 Mev.

TABLE V. Validity of method of Cu control activity.

Nucleus	Threshold h.u.	Cu control (c/r)	Diff. in threshold Cu control	Actual diff. in thresholds (h.u.)
Cu^{63}	674	480	4.8	5
Cu^{63}	669	565		
Ag^{109}	560	520	8.0	9
Ag^{109}	551	680		
N^{14}	669	480	11.5	10
N^{14}	659	710		
O^{16}	1040	480	11.5	6
O^{16}	1034	710		
C^{12}	1243	480	11.5	11
C^{12}	1232	710		

the helipot correction method based on the Cu control activity can be expected to be much more precise. In fact, consideration of the results on the reproducibility of Cu activations indicated a precision of the order of ± 0.4 h.u.

VIII. NONLINEARITY OF ENERGY SCALE

There are many factors which could contribute to a nonlinearity in the helipot setting *versus* peak x-ray energy curve. Among these, two of the more likely hypotheses were: (1) a time delay between the instant when electron orbit expansion is initiated and the time at which it actually occurs, and (2) the possibility of a phase shift between the flux integrator amplifier input signal and the magnetic field.

An experiment was performed in order to determine the presence of such effects. A set of runs was taken at constant helipot setting, but at different settings of the peak magnet amplitude. It is evident that this corresponds to expanding the beam at different values of rate of change of magnetic flux. An additional complication is present in that the response of the integrator amplifier may also be dependent on the rate of change of voltage at the voltage level (helipot setting) at which orbit expansion is called for.

The results of such an experiment showed that at helipot 730 a change in magnet amplitude of from 11 to 21 Mev produced a change in the Cu activity which was equivalent to a shift in the peak x-ray energy of about 22 h.u. (300 kev). It was found that these results were consistent with the assumption of a constant time delay. However, when a correction based upon these results was applied to the calibration points for the energy scale, the resulting scale possessed a nonlinearity which was roughly the same as that which it had originally. It therefore appeared that the above considerations would not resolve the scale nonlinearity.

A conclusion of practical utility could be obtained from this experiment, namely, the degree to which the magnet amplitude must be held constant in order to eliminate this as an effect causing fluctuations in the peak x-ray energy. In the neighborhood of magnet amplitude 21 Mev, a 1-Mev change in the magnet amplitude can produce a change in the peak x-ray energy of 28 kev. Thus, if a stability of the order of ± 3 kev is desired, the magnet amplitude must be held constant to within ± 0.1 Mev.

ACKNOWLEDGMENTS

It is a pleasure to thank Professor Jules R. de Launay for his supervision of this work; Dr. Leo Seren, not only for suggesting the problem, but also for helpful guidance; Dr. Erich M. Harth for many stimulating discussions and helpful suggestions; Dr. Warren L. Bendel for carefully reading the manuscript and suggesting numerous improvements; Mr. Ralph A. Tobin for maintaining the betatron; Dr. F. N. D. Kurie for his support; and the entire U. S. Naval Research Laboratory organization for their generous cooperation.